ELSEVIER

Journal of Photochemistry and Photobiology A: Chemistry 117 (1998) 111–117

Journal of Photochemistry and Photobiology A:Chemistry

Photoinduced electron transfer from indolic compounds to 1-pyrenemethanol in polystyrene latex dispersions

Kenichi Nakashima[a,*], Senri Tanida[a], Tsuyoshi Miyamoto[a], Shuichi Hashimoto[b]

[a] *Department of Chemistry, Faculty of Science and Engineering, Saga University, 1 Honjo-machi, Saga 840-8502, Japan*
[b] *Department of Chemistry, Gunma College of Technology, 580 Toriba-machi, Maebashi, Gunma 371-0845, Japan*

Received 28 January 1998; received in revised form 8 May 1998; accepted 23 June 1998

Abstract

Photoinduced electron transfer from indolic compounds to 1-pyrenemethanol (PyM) in polystyrene latex dispersions has been studied by steady-state and time-resolved fluorescence spectroscopy. The photoinduced electron transfer reaction is observed by monitoring fluorescence quenching of PyM. The indolic compounds employed are tryptamine (Trm) and tryptophan (Trp). From steady-state fluorescence measurements, it is found that the photoinduced electron transfer from Trm to PyM is remarkably enhanced on going from the aqueous homogeneous solution to the latex dispersion, while no such latex effect is observed for the Trp–PyM pair. This is attributed to the fact that Trp is not effectively adsorbed onto the latex particles in contrast to Trm and PyM, as evidenced by the measurement of respective adsorption isotherms. Fluorescence decay curves of PyM in polystyrene latex dispersions are successfully analyzed in terms of two-exponential functions. The analysis reveals that quenching of PyM fluorescence by Trm (i.e., photoinduced electron transfer from the latter to the former) on polystyrene latex surfaces is mainly operated by a static mechanism.

Keywords: Electron transfer; Fluorescence; 1-Pyrenemethanol; Tryptamine; Tryptophan; Polystyrene latex

1. Introduction

Latex particles represent a new type of organic solid material which can be employed as a micro-substrate for photoreactions. The surface consists of organic polymers embedded sparsely with functional groups such as sulfate, carboxyl, or amino groups. This structure leads latex particles to have two kinds of adsorption sites on the surface: (1) the polymer matrix which affords continuous adsorption domains to non-polar and less polar adsorbates, and (2) the functional group which gives discrete adsorption points to ionic and highly polar species. Such a feature has never been seen in any of the other solid materials. Furthermore, latex particles have many other features as follows: (a) various kinds of functional groups can be introduced onto the latex surfaces; (b) concentration of the functional groups on latex surfaces can be easily controled by modern synthesis techniques; (c) different types of polymers such as polystyrene (PS) and polyacrylates, with varying degrees of polarity can be employed as the support material; (d) the particle shape is highly uniform (spherical); (e) the particle size can be controlled within a narrow distribution.

*Corresponding author. Tel.: +81-952-28-8850; fax: +81-952-28-8548; e-mail: nakashik@cc.saga-u.ac.jp

We have investigated several photoreactions on the surface of PS and poly (butyl methacrylate) latexes in aqueous dispersions. Photoreactions so far investigated include electronic energy transfer from rhodamine dyes to malachite green [1,2], photoinduced electron transfer from 1-pyrenemethanol to methylviologen [3], and excimer formation of pyrene derivatives [4]. We find that on going from a homogeneous aqueous solution to the latex dispersion, the efficiencies of the photoreactions are dramatically enhanced. In this paper, we report studies of photoinduced electron transfer (PET) from indolic compounds to 1-pyrenemethanol (PyM) on the surface of PS latex in aqueous dispersions. The indolic compounds employed are tryptamine (Trm) and tryptophan (Trp).

It is known that the fluorescence of pyrene family (PyX) is quenched by indolic compounds (Ins) through PET as shown in Scheme 1. [5–9] according to Scheme 1, we observed the PET reaction by monitoring the fluorescence quenching of PyM. From steady-state fluorescence measurements, it is found that the PET from Trm to PyM is remarkably enhanced on going from the aqueous homogeneous solution to the latex dispersion, while no such latex effect is observed for the Trp–PyM pair. The difference is discussed based on the adsorption isotherms of the donors and acceptor onto the

1010-6030/98/$ – see front matter
PII: S1010-6030(98)00331-1

$$PyX + h\nu_a \rightarrow PyX^*$$

$$PyX^* + In \xrightarrow{PET} PyX^{\bullet -} + In^{\bullet +}$$

$$\downarrow \text{Fluorescence}$$

$$PyX + h\nu_f$$

Scheme 1.

latex particles. Time-resolved fluorescence studies reveal that PET from Trm to PyM on PS latex surfaces is mainly operated by a static mechanism [10,11].

2. Experimental details

PyM (Molecular Probes) was used as received. Trp and tryptamine hydrochloride (Trm·HCl) from Tokyo Kasei Kogyo were guaranteed grade, and used without further purification. Structural formulae of these compounds are shown in Fig. 1. Water was purified with a Millipore Milli Q purification system.

Styrene monomer was washed with 2% sodium hydroxide solution, followed by vacuum distillation. The PS latex was synthesized by standard emulsion polymerization in the presence of sodium dodecyl sulfate [1]. The latex was repeatedly dialyzed against water until the conductivity of the serum was reduced to that of Milli Q water. Diameter of the latex particles was determined with an Otsuka DLS-7000 dynamic light scattering spectrophotometer. The mean diameter is 182 nm with a narrow size distribution.

Stock solutions of the donors and acceptor in water were prepared to give concentrations of 100 mM and 10 μM, respectively. PyM is completely dissolved in water at the concentration of 10 μM. Aliquots of the PS dispersion and donor/acceptor stocks were mixed in a 10 ml volumetric flask, followed by sonication for 5 min. The samples were stored in the dark for 1 day before the spectroscopic measurements. In fluorescence experiments, the samples were deaerated by nitrogen-purging for 15 min unless otherwise mentioned.

Adsorption isotherms of PyM, Trp, and Trm onto the latex surface were measured by ultracentrifugation. Aliquots of the latex dispersion containing known amounts of the probe were placed in ultracentrifuge tubes, and centrifuged with Beckman Avanti-30 ultracentrifuge for 60 min at 26×10^3 rpm (57×10^3 *g*). Concentration of the probe in the supernatant after centrifugation was determined by UV absorption. The amount of the probe adsorbed was calculated from the difference of the total concentration in the dispersion and equilibrium concentration in the serum.

Fluorescence spectra were recorded on a Hitachi F-4000 spectrofluorometer. Spectra were corrected by the use of a standard tungsten lamp with a known color temperature. Steady-state fluorescence intensity is expressed in terms of peak height of a band at around 395 nm, unless otherwise stated. Absorption spectra were measured with a Jasco Ubest-50 spectrophotometer. Fluorescence lifetime measurements were carried out with a Horiba NAES 1100 time-resolved spectrofluorometer which employs a time-correlated single photon counting technique.

Electron Donor:

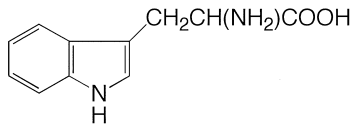

Tryptophan (Trp)

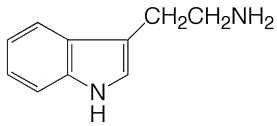

Tryptamine (Trm)

Electron Accepter:

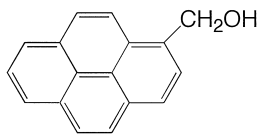

1-Pyrenemethanol (PyM)

Fig. 1. Structural formulae of electron donors and an acceptor.

3. Results and discussion

3.1. Steady-state fluorescence study

We observed fluorescence spectra of PyM in the absence and presence of Trp (data not shown). Quenching of the PyM fluorescence by Trp was not much affected by the existence of PS latex particles; this D–A pair gives similar Stern–Volmer plots for an aqueous solution and a PS latex dispersion ([Trp]=0∼5 mM). The Stern–Volmer constants obtained are 460 M^{-1} for the aqueous solution and 410 M^{-1} for the latex dispersion. Using a lifetime data (τ_f=190 ns) obtained by us earlier [3], we calculate the quenching rate constant for an aqueous solution: $k_q=2.4\times10^9$ M^{-1} s^{-1}. This value is close to that ($k_q=2.2\times10^9$ M^{-1} s^{-1}) reported by Encinas and Lissi [6] for a Trp–pyrene pair in an aqueous solution at pH 7.

The insignificant effect of the latex particles on PET from Trp to PyM is attributed to that little Trp is adsorbed onto the latex particles as confirmed by the adsorption isotherm. The pH value of aqueous solution of Trp varies from 6.1 to 6.4 corresponding to its concentration from 0.5 to 5 mM. Over

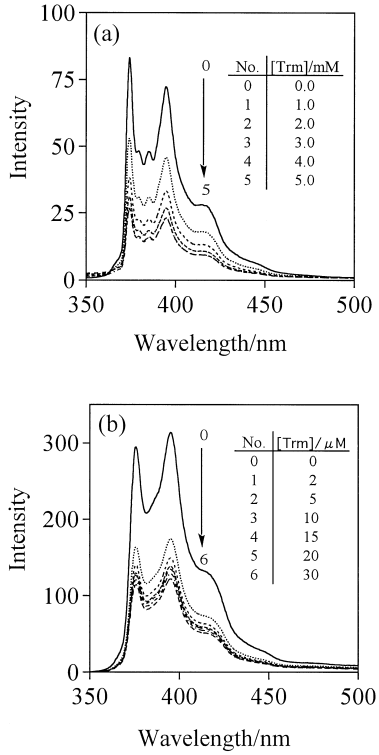

Fig. 2. Fluorescence spectra of PyM in the absence and presence of Trm. (a) Aqueous solution: [PyM]=1.0 μM; the samples are excited at 325 nm; excitation and emission bandpasses are 10 and 1.5 nm, respectively. (b) PS latex dispersion: [PyM]=2.0 μM; [PS]=1.15 g l^{-1}; the samples are excited at 325 nm; excitation and emission bandpasses are 3 and 5 nm, respectively.

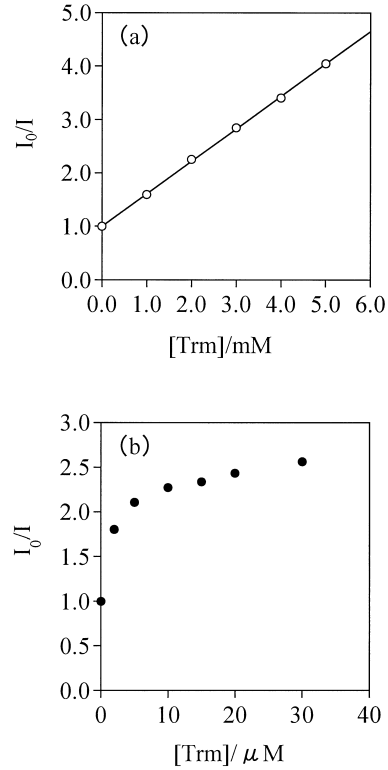

Fig. 3. Stern–Volmer plots for the systems in Fig. 2: (a) aqueous solution; (b) PS latex dispersion.

this pH region, Trp exists almost in a zwitter-ionic form as calculated from its isoelectric point (5.89). Therefore, it seems that electrostatic attraction between Trp and the sulfate groups on the PS latex surface is not effective for Trp adsorption, nor is hydrophobic interaction between Trp and PS matrices of the latex.

In contrast to Trp–PyM case, PyM fluorescence is markedly quenched by Trm on going from an aqueous homogeneous solution to a PS latex dispersion (Fig. 2). It is noted from Fig. 2 that the quenching in the latex dispersion is effectively brought about even when Trm concentration is lowered to 2 μM which is 1000 times smaller than that needed for the quenching in aqueous solutions. This means that PET in the latex dispersions takes place about 1000 times more efficiently than that in aqueous solutions. The marked enhancement of PET can be ascribed to the increase in local concentrations of the donor and acceptor on the latex surface, as confirmed by the measurements of the adsorption isotherms (data shown later). Trm employed is hydrochloride, and the pH value of the aqueous solution is around 6 over the concentration range in Fig. 2(b). At this pH, Trm exists almost in a cationic form because its pK_b is 3.8. Thus, electrostatic attraction between Trm and sulfate groups on the latex surface seems to play a main role in Trm adsorption.

In Fig. 3, we show plots of PyM fluorescence intensity against Trm concentration in an aqueous homogeneous solution and a PS latex dispersion. The plot for the aqueous solution is linear, giving a Stern–Volmer constant of 630 M^{-1}. The quenching rate constant is 3.3×10^9 M^{-1} s^{-1}, which is comparable to that of Trp–PyM pair. In contrast to the plot for the aqueous solution, the one for the latex dispersion show a downward curve. Such downward-curving plots were investigated by Eftink and Ghiron [12,13] for various cases. According to them, a downward curving plot is obtained when a fluorophore is distributed in two or more different environments which have different accessibility to fluorescence quenching (*heterogeneously emitting system*). If we denote two environments as, a and b, quantitative expression for the relation between fluorescence intensity and quencher concentration ([Q]) is given by the following equation [12,13]:

$$\frac{I_0}{I} = \left[\frac{f_a}{(1+K_a[Q])\exp(V_a[Q])} + \frac{f_b}{(1+K_b[Q])\exp(V_b[Q])}\right]^{-1} \quad (1)$$

$$f_a = I_{0a}/(I_{0a}+I_{0b}) = I_{0a}/I_0, \quad f_b = I_{0b}/(I_{0a}+I_{0b}) = I_{0a}/I_0 \quad (2)$$

where I_0 and I denote the total fluorescence intensities of a fluorophore in the absence and presence of the quencher, respectively. I_{0i} (i=a and b) represents the contribution of I_0 from the component in the environment i. K_i and V_i (i=a and

b) are dynamic and static quenching constants for the fluorescent component *i*. By simulation, Eftink and Ghiron showed that the plot of I_0/I versus $[Q]$ becomes a downward curve when the following condition is fulfilled: $(K_a+V_a)\geq 4(K_b+V_b)$.

In our latex systems, it is difficult to analyze the downward curve (Fig. 3(b)) in terms of Eq. (1) because this equation contains too many parameters to be determined. Therefore we consider one of the simplest cases, which was proposed by Lehrer [14]. According to Lehrer, we obtain Eq. (3) by assuming that $K_b=V_b=V_a=0$ in Eq. (1):

$$I_0/(I_0 - I) = 1/f_a K_a[Q] + 1/f_a \quad (3)$$

It should be noted here that $\exp(V_a[Q])$ in Eq. (1) is approximately equal to $1+V_a[Q]$ when $V_a[Q]$ is much smaller than unity. Under such conditions Eq. (3) is valid even if the quenching in the environment a is operated by static mechanism (i.e., $K_a=0$, $V_a\neq 0$). We plot $I_0/(I_0-I)$ against 1/[Trm] in Fig. 4, where the total concentration of Trm in the latex dispersion is employed instead of the local concentration on the latex surface because the quencher is probably distributed two-dimensionally on the latex surface. The plot in Fig. 4 shows a linearity to some extent between $I_0/(I_0-I)$ and 1/[Trm], although the treatment is too simplified. From the intercept and the slope, we obtained $f_a=0.61$ and $K_a=1.3\times 10^6\ M^{-1}$. This Stern–Volmer constant is apparent and does not have its original meaning, because the quencher concentration is expressed by a total concentration in the dispersion despite the fact that quenching mostly takes place on the latex surface. Thus, the extraordinarily large value of K_a reflects the increase in the local concentration of the quencher on the latex surface. However, if we consider the K_a value as a measure of concentrating effect of the latex surface on the reactants, we can realize that the PET reaction is remarkably enhanced on going from an aqueous solution ($K_a=630\ M^{-1}$) to the latex dispersion ($K_a=1.3\times 10^6\ M^{-1}$).

It is necessary for us to get an insight into the environments a and b for substantiating the above analysis. The accessible environment a is probably the surface of the latex particles, which is exposed to water. As for the inaccessible site b, there seems to be two candidates: (i) some kind of hole inside the latex particles, which PyM can diffuse in but Trm can not, and (ii) an aqueous phase where the quenching of PyM fluorescence by Trm is inefficient at such low concentrations as several tens μM. First we consider the case (ii). In this case, the population of PyM on the latex surface should be close to f_a (=0.61) under the assumption that the quantum yield of PyM does not much change on going from aqueous phase to the latex surface (see Eq. (2)). We observed an adsorption isotherm of PyM onto the latex particles (Fig. 5(a). The horizontal axis of Fig. 5(a) represents the total concentration of PyM in the latex dispersion, and the vertical axis does the concentration of adsorbed PyM, which is calculated as the difference between the total concentration in the dispersion and the equilibrium concentration in the supernatant. Accordingly, the slope of the line in Fig. 5(a) gives the mole fraction of PyM on the latex particles. We see from Fig. 5(a) that 89% of PyM exists on the latex particles. This value (0.89) is 1.5 times larger than the value of f_a (0.61) obtained from Fig. 4. This difference may be partly formed from the roughness of the treatment yielding Eq. (3). As another cause of the difference, we take the case (i) into account; we consider that a portion of PyM molecules on the latex particles is accommodated in some

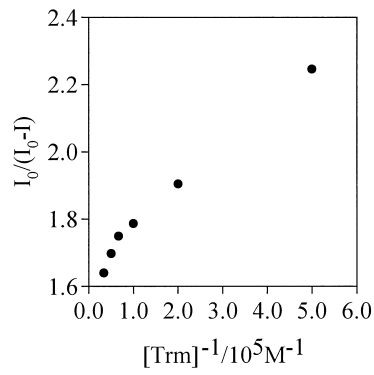

Fig. 4. Modified Stern–Volmer plot for the systems in Fig. 2(b).

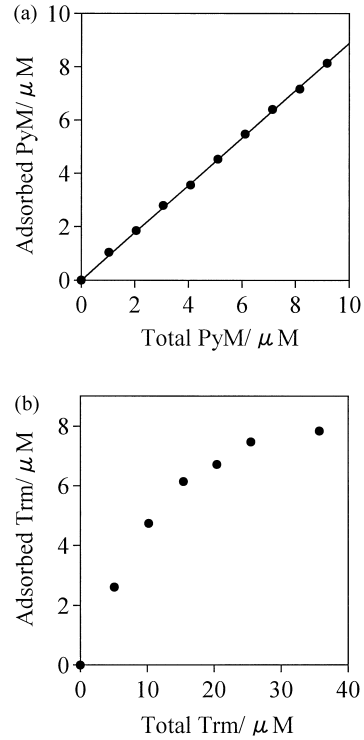

Fig. 5. Adsorption isotherms of (a) PyM and (b) Trm onto PS latex particles at 20°C. [PS]=1.15 g l^{-1}. The horizontal axis represents the total concentration of PyM in the latex dispersion, and vertical axis the concentration of adsorbed PyM. Accordingly, the slope of the line gives the mole fraction of PyM adsorbed on the latex particles. It should be noted here that the concentrations of PyM and Trm in these experiments are lower than those for saturating the adsorption.

hole, in which PyM can diffuse but Trm can not. In this situation, PyM molecules in the hole is not accessible to quenching although they are adsorbed onto the latex particles. If we remember that Trm exists almost in a cationic form under the experimental condition, it is likely that there is a hydrophobic hole inside the latex particles, which PyM can diffuse in but Trm can not due to its ionic nature. In conclusion, both of the cases (i) and (ii) seem to explain the present inaccessible site b. It should be noted here that the difference between the two values (0.61 and 0.89) cannot be attributed to the breakdown of the assumption that the quantum yield of PyM is not much affected by the latex surface. The quantum yield of PyM is, actually, affected by the latex surface. However, the quantum yield is increased on going from aqueous phase to the latex surface, which will lead to a f_a value larger than the mole fraction on the latex surface. This is a tendency opposite to the observed result.

We present an adsorption isotherm of Trm onto the latex particles in Fig. 5(b), where the total concentration of Trm is varied in almost the same range as in Fig. 3(b). As we can see, the adsorption isotherm is downward curving. This indicates that the adsorption coefficient of Trm decreases with increasing total concentration, so that the local concentration of Trm on the latex surface does not linearly increase with the total concentration. Therefore, the downward-curving nature in Stern–Volmer plot for the latex systems (Fig. 3(b)) seems to be ascribed, in part, to this adsorption behavior of Trm. However, if we compare Fig. 5(b) with Fig. 3(b), we note that the profiles of the two downward curves are different. The Stern–Volmer plot (Fig. 3(b)) shows a steep rise in low Trm concentration region ($\leq$10 μM), whereas the adsorption isotherm (Fig. 5(b)) is almost linear at this concentration region. Thus, the low Trm concentration region of the downward-curving Stern–Volmer plot seems to be explained by the model of *heterogeneously emitting system*, as already discussed. As to the high Trm concentration region ($\geq$10 μM), both the heterogeneously emitting PyM and the decreasing adsorption coefficient of Trm might be responsible for the downward deviation of the Stern–Volmer plot.

3.2. Time-resolved fluorescence study

In order to obtain an insight into the mechanism of quenching of PyM fluorescence by Trm, we observed the fluorescence decay curves (Fig. 6). It turned out that the decay curves of PyM in the latex dispersion are conformed to a two-exponential function even when Trm is absent:

$$I(t) = A_1 \exp(-t/\tau_1) + A_2 \exp(-t/\tau_2) \quad (4)$$

where τ_1 and τ_2 denote the lifetime of each component, and A_1 and A_2 are pre-exponential factors. Here it is of value to point out that integration of each term in Eq. (4) with respect to time t gives a relative quantum yield (y_i) of the corresponding component:

$$y_i = \int A_i \exp(-t/\tau_i)\mathrm{d}t = A_i\tau_i \quad (\text{for } i = 1 \text{ and } 2). \quad (5)$$

For convenience of later discussion, we define a total quantum yield (Y) as:

$$Y = y_1 + y_2 = A_1\tau_1 + A_2\tau_2 \quad (6)$$

We obtained, from Fig. 6(a), τ_1=94.2 ns (A_1=0.137) and τ_2=234 ns (A_2=0.262). The two component nature of the decay curve seems to be ascribed to the fact that PyM is partitioned in two different milieus; one (τ_1) is derived from the species in an aqueous phase and the other (τ_2) is from those on the latex particle. This assignment is supported by comparison of y_2 with Y. As calculated from the above data, the ratio y_2/Y is 0.83, which is close to the mole fraction of PyM on the latex particle (0.89).

An analysis of decay component is quite useful for obtaining information about whether the quenching is *dynamic* or *static* [10,11]. In dynamic quenching, τ_i is decreased with increasing quencher concentration, while

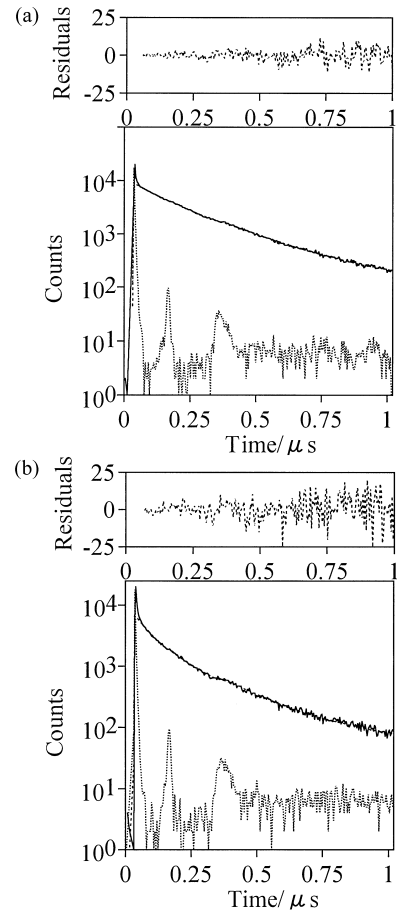

Fig. 6. Fluorescence decay curves of PyM in PS latex dispersions: (a) in the absence of Trm, (b) in the presence of Trm (10 μM). [PyM]=2.0 μM, [PS]=1.15 g/l. The samples are excited at 325 nm and the excitation bandpass is 14 nm. The emission is collected through a Toshiba L-37 cut-off filter.

A_i is not changed, as seen from the well-known Stern–Volmer equation [10,11]:

$$y_{i0}/y_i = A_{i0}\tau_{i0}/A_i\tau_i = \tau_{i0}/\tau_i = 1 + K_{SV}[Q] \quad (7a)$$

$$A_{i0}/A_i = 1 \quad (7b)$$

where the subscript 0 denotes the absence of a quencher. In static quenching, on the other hand, A_i is decreased with increasing quencher concentration, while τ_i remains constant:

$$y_{i0}/y_i = A_{i0}\tau_{i0}/A_i\tau_i = A_{i0}/A_i = 1 + K_S[Q] \quad (8a)$$

$$\tau_{i0}/\tau_i = 1 \quad (8b)$$

Before we discuss the details of the component analysis, it should be noted that the reliability of data on the shorter component 1 is somewhat low due to the interference by scattered excitation light. This is often a problem for solid polymer systems, as pointed out by Kaneko et al. [15]. Therefore, we will not be much concerned with the shorter component. As the contribution of the shorter component to the total fluorescence intensity is small (~0.17), the low reliability of the data on this component does not seriously influence the following discussion. In Fig. 7, we plot A_2, τ_2, and y_2 as a function of Trm concentration. As seen from Fig. 7, the A_2 value is drastically decreased (from 0.262 to 0.0951) when Trm concentration is increased from 0 to 30 μM, whereas τ_2 is slightly decreased (from 234 to 203 ns). These large changes in A_2 and small change in τ_2 suggest that the quenching of component 2 is operated by a static mechanism. In contrast, the quenching of the shorter component 1 seems to be dominated by a dynamic process because τ_1 is significantly decreased with increasing Trm concentration, while A_1 is not much affected (data not shown).

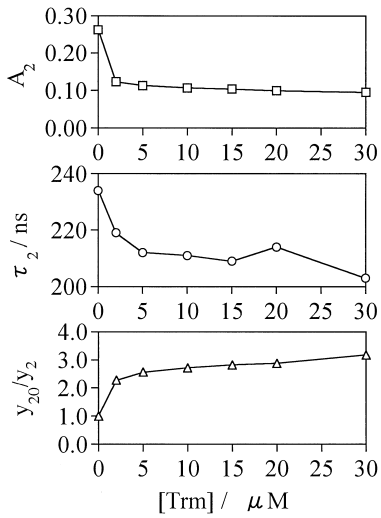

Fig. 7. Lifetime (τ_2) and pre-exponential factor (A_2) of the component 2 of PyM fluorescence as a function of Trm concentration in a PS latex dispersion. [PyM]=2.0 μM, [PS] =1.15 g/l. The value y_{20}/y_2 is also plotted against Trm concentration, where y_{20} and y_2, respectively, are relative emission quantum yields of the component 2 in the absence and presence of Trm.

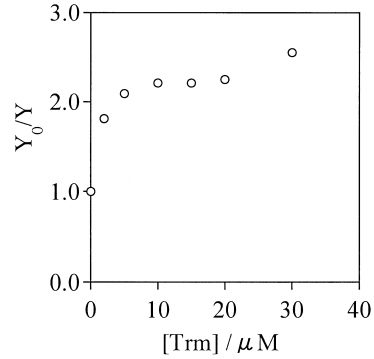

Fig. 8. Plot of Y_0/Y versus [Trm] obtained from time-resolved fluorescence measurements for the same systems as in Fig. 3(b). Y_0 and Y are the total fluorescence quantum yields of PyM in the absence and presence of Trm, respectively (see Eq. (6)).

In Fig. 8, we plot Y_0/Y against [Trm]. As Y_0 and Y is total quantum yields of PyM fluorescence (see Eq. (6)) in the absence and presence of the quencher, respectively, the plot in Fig. 8 corresponds to the one in Fig. 3(b). It should be noted that I_0/I (Fig. 3(b)) and Y_0/Y (Fig. 8) show quite similar dependence on the quencher concentration, although the former is obtained from steady-state fluorescence measurements while the latter is from time-resolved experiments. This similarity assures the reliability of the present two measurements.

4. Conclusions

We have shown from steady state fluorescence measurements that PET from Trm to PyM is enhanced about one thousand times on going from the aqueous homogeneous solution to the PS latex dispersion. This is attributed to increase in local concentrations of both Trm and PyM on the latex surface, as evidenced by their adsorption isotherms. The Stern–Volmer plot for Trm–PyM in the aqueous solution is linear, giving a PET quenching rate constant of $3.3\times10^9\ M^{-1}\ s^{-1}$, while the plot for the same pair in the latex dispersion becomes downward-curving. The downward curve is explained, in part, by a model of *heterogeneously emitting system* [12–14], which assumes the distribution of a fluorophore in two environments: one is accessible to quenching and the other is not. The change of adsorption coefficient of Trm onto the latex particles is also responsible for the deviation of the Stern–Volmer plot from linearity. In contrast to the Trm–PyM case, there is no significant enhancement of PET for a Trp–PyM pair in the latex dispersion. It is elucidated from adsorption isotherm measurements that Trp is not efficiently adsorbed onto the latex surface. The Stern–Volmer plots for this pair are linear both in the aqueous solution and in the latex dispersion. The PET quenching rate constant of Trp–PyM

pair in the aqueous solution is $2.4\times10^9\ M^{-1}\ s^{-1}$, which is close to $2.2\times10^9\ M^{-1}\ s^{-1}$ reported by Encinas and Lissi [6].

The mechanism of PET quenching of the Trm–PyM pair in the latex dispersion has been examined by time-resolved fluorescence measurements. The fluorescence decay curve of PyM shows two-exponential nature in the latex dispersion, reflecting the distribution of this fluorophore between bulk aqueous phase and the latex particles. From the dependence of decay profiles of PyM fluorescence on Trm concentration, it is elucidated that the PET quenching on the latex surface is operated by a static mechanism [10,11].

There are, generally, two purposes in employing solid surfaces as reaction media for PET reactions: (1) to perform effective electron transfer and (2) to suppress back electron transfer to elongate charge-separated states [16]. In the present study, we found that the PS latex system is useful for accomplishing the purpose (1). The next step is to examine the latex system for the purpose (2). One of the products of the present PET reaction, $PyM^{\bullet-}$ anion (see Scheme 1), seems to be repelled from the latex surface due to electrostatic repulsion between this species and the sulfate groups on the latex surface. On the other hand, the other product $In^{\bullet+}$ cation will be fixed to the sulfate groups on the latex surface by electrostatic attraction. Therefore, we expect that recombination of the products will be prevented by the latex particles. This can be confirmed by monitoring the transient absorption of the products. Such an investigation is now in progress using diffuse-reflectance laser flash photolysis techniques [17].

Acknowledgements

The authors thank Professor Takuji Tsukamoto (Saga University) for the use of their time-resolved spectrofluorometer. The present work is partly defrayed by the Grant-in-Aid for Scientific Research on Priority-Area-Research 'Photoreaction Dynamics' from the Ministry of Education, Science, Sports, and Culture of Japan (No. 08218249).

References

[1] K. Nakashima, J. Duhamel, M.A. Winnik, J. Phys. Chem. 97 (1993) 10702.
[2] K. Nakashima, Y.S. Liu, P. Zhang, J. Duhamel, J. Feng, M.A. Winnik, Langmuir 9 (1993) 2825.
[3] K. Nakashima, N. Kido, Photochem. Photobiol. 64 (1996) 296.
[4] K. Nakashima, N. Kido, A. Yekta, M.A. Winnik, J. Photochem. Photobiol. A: Chem. 110 (1997) 207.
[5] J.P. Palmans, M. Van der Auweraer, A.M. Swinnen, F.C. De Schryver, J. Am. Chem. Soc. 106 (1984) 7721.
[6] M.V. Encinas, E.A. Lissi, Photochem. Photobiol. 44 (1986) 579.
[7] O.E. Zimerman, J.J. Cosa, C.M. Previtali, Photochem. Photobiol. 52 (1990) 5711.
[8] H.A. Montejano, J.J. Cosa, H.A. Garrera, C.M. Previtali, J. Photochem. Photobiol. A: Chem. 86 (1995) 115.
[9] C.D. BorsarelliH, H.A. Montejano, J.J. Cosa, C.M. Previtali, J. Photochem. Photobiol. A: Chem. 91 (1995) 13.
[10] J.B. Birks, Photophysics of Aromatic Molecules, Wiley-Interscience, London, UK, 1970.
[11] J.R. Lakowicz, Principles of Fluorescence Spectroscopy, Plenum, New York, 1986.
[12] M.R. Eftink, C.A. Ghiron, Biochemistry 15 (1976) 672.
[13] M.R. Eftink, C.A. Ghiron, Anal. Biochem. 114 (1981) 199.
[14] S.S. Lehrer, Biochemistry 10 (1971) 3254.
[15] K. Nagai, J. Tsukamoto, N. Takamiya, M. Kaneko, J. Phys. Chem. 99 (1995) 6648.
[16] K. Kalyanasundaram, Photochemistry in Microheterogeneous Systems, Academic Press, New York, 1987.
[17] S. Hashimoto, Chem. Phys. Lett. 252 (1996) 236.